THE JOURNAL OF PHYSICAL CHEMISTRY C

Article

pubs.acs.org/JPCC

Lithium Polysulfide Radical Anions in Ether-Based Solvents

Kevin H. Wujcik,[†,§] Dunyang Rita Wang,[‡,§] Aditya Raghunathan,[†,§] Melanie Drake,[†] Tod A. Pascal,[∥] David Prendergast,[∥] and Nitash P. Balsara*[,†,§,⊥]

[†]Department of Chemical and Biomolecular Engineering and [‡]Department of Materials Science and Engineering, University of California, Berkeley, California 94720, United States

[§]Materials Sciences Division, [∥]Molecular Foundry, and [⊥]Environmental Energy Technologies Division, Lawrence Berkeley National Laboratory, Berkeley, California 94720, United States

Supporting Information

ABSTRACT: Lithium sulfur batteries have a theoretical specific energy 5 times greater than current lithium ion battery standards, but suffer from the issue of lithium polysulfide dissolution. The reaction mechanisms that underlie the formation of lithium polysulfide reaction intermediates have been studied for over four decades, yet still elude researchers. Polysulfide radical anions formed during the redox processes have become a focal point of fundamental Li−S battery research. The formation of radical species has even been shown to be advantageous to the electrochemical pathways. However, whether polysulfide radical anions can form and be stabilized in common Li−S battery electrolytes that are ether-based is a point of contention in Li−S battery research. The goal of this work was to examine the presence of radical polysulfide species in ether-based solvents. Lithium polysulfide solutions in tetraethylene glycol dimethyl ether and poly(ethylene oxide) are probed using a combination of ultraviolet−visible (UV−vis) and electron paramagnetic resonance (EPR) spectroscopy. EPR results confirm the presence of radical species in ether-based electrolytes. Comparison of the UV−vis spectra to EPR spectra establishes that the UV−vis absorbance signature for radical species in ether-based solvents occurs at a wavelength of 617 nm, which is consistent with what is observed for high electron pair donor solvents such as dimethylformamide and dimethyl sulfoxide.

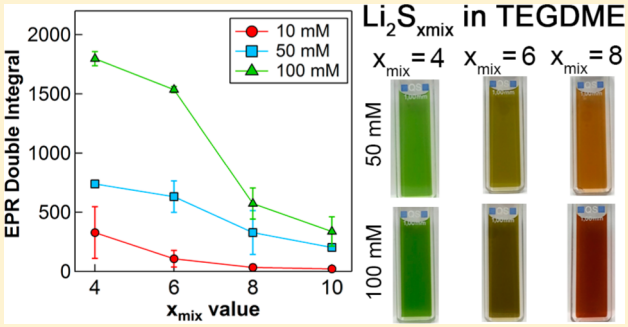

INTRODUCTION

Lithium sulfur (Li−S) batteries are attractive for energy storage applications because they have a theoretical specific energy of 2600 (W h)/kg, and because sulfur is affordable and naturally abundant.[1] Unfortunately, Li−S cells are plagued by issues related to the dissolution of reaction intermediates, collectively called lithium polysulfides, that are formed during charge and discharge. As the redox reactions proceed, these polysulfides dissolve in the electrolyte and diffuse out of the cathode, causing the battery capacity to fade. Additionally, if diffusion to the cell anode occurs, polysulfides may react with lithium, forming insulative layers of Li_2S and Li_2S_2, and leading to parasitic shuttles if soluble species are formed.[2−4]

While lithium polysulfide molecules are most commonly thought to be dianion species (Li_2S_x, $2 \le x \le 8$),[5,6] evidence of polysulfide radical anions (LiS_x, $3 \le x \le 5$) in Li−S batteries has also been obtained.[7−11] Recent studies have even suggested that radical anions may be of benefit to Li−S reaction pathways.[10,11] It has been argued that the presence of radical species (here we refer to polysulfide radical anions as radicals or radical species for simplicity) in a particular lithium sulfur cell depends primarily on the electron pair donor (EPD) number of the electrolyte.[12,13] Solvents with high EPD numbers may stabilize radical polysulfides, while solvents with low EPD numbers do not.

The long-term stability of polysulfide radicals in some environments is well-established. This is demonstrated most clearly by lapis lazuli, a blue mineral that is pulverized to form a pigment commonly known as ultramarine. Through extensive studies involving electron paramagnetic resonance (EPR) spectroscopy, Raman spectroscopy, ultraviolet−visible (UV−vis) light spectroscopy, and X-ray absorption spectroscopy (XAS), the blue color of ultramarine/lapis lazuli has been attributed to the $S_3^{\bullet-}$ trisulfur radical anion.[14−16] The crystalline tectosilicate cage structure of the mineral stabilizes the radical anion, apparently isolating the individual molecules and preventing recombination of these reactive species. Additional studies on the chemical composition of ultramarine/lapis lazuli suggest that $S_2^{\bullet-}$ may also be present.[17] The $S_3^{\bullet-}$ radicals that give the blue color of ultramarine pigments have been stable for thousands of years.

Polysulfide radicals have been reported to be stable in solvents such as DMF and DMSO that have high EPD

Received: April 27, 2016
Revised: July 4, 2016
Published: August 11, 2016

DOI: 10.1021/acs.jpcc.6b04264
J. Phys. Chem. C 2016, 120, 18403−18410

numbers. Radical species such as LiS_3 and LiS_4 were detected in equilibrium with dianion species (e.g., Li_2S_6) in these systems by XAS, EPR spectroscopy, and UV−vis absorbance spectroscopy.[3,12,18−34] Solutions of polysulfide species in solvents with high EPD numbers are typically blue in color, owing to the presence of LiS_3.[3,12,18,23]

It is not clear if polysulfide radicals are present in solvents with low EPD numbers, such as dimethyl ether (DME), 1,3-dioxolane (DOL), tetraethylene glycol dimethyl ether (TEGDME), and poly(ethylene oxide) (PEO). Some studies indicate the presence of radicals in these ether-based systems,[7−9,11,13] while others do not.[10,35−40] Establishing the stability of radicals in these ether-based electrolytes is important because these solvents are often used in Li−S cells.[5,7,8,35,40−42]

In this study, we quantify the presence of radicals in chemically synthesized lithium polysulfides in TEGDME and PEO using a combination of UV−vis and EPR spectroscopy. Our results provide unambiguous proof of the existence of radical anions in these solvents, and show that the concentration of radical species is a complex function of the polysulfide type and concentration. On the basis of the observed EPR *g* factors, the identification of the radical species present in the ether-based solvents is discussed, but further work is needed to confirm the exact radical species present in solutions.

EXPERIMENTAL SECTION

Materials. Lithium sulfide (Li_2S) and elemental sulfur (S_8) were purchased from Alfa Aesar and were received under argon. Tetraethylene glycol dimethyl ether (TEGDME) (99.0%) was purchased from Sigma-Aldrich and was obtained under argon. Poly(ethylene oxide) (PEO), also referred to as poly(ethylene glycol), was purchased from Polymer Source Inc. and had a molar mass of 600 g/mol. The PEO was dried overnight at 90 °C under vacuum and then brought into the glovebox. All materials were stored in an argon-filled glovebox.

Lithium Polysulfide Solutions. Lithium polysulfide solutions were prepared by adding stoichiometric amounts of S_8 and Li_2S to the solvent of interest as described by Rauh et al.[3] The amounts of S_8 and Li_2S added to solutions were controlled by the following formula:

$$Li_2S + \frac{x_{mix} - 1}{8} S_8 \rightarrow Li_2S_{x_{mix}} \quad (1)$$

Here x_{mix} is used to denote the polysulfide dianion that would be obtained if a single dianion polysulfide type were formed by the reaction. In reality, the solution is likely a mixture of various polysulfide species in equilibrium, formed through various disproportionation reactions. This distribution of polysulfide species can include both dianions (of the form Li_2S_x) and radical species (of the form LiS_x).[3] Here x_{mix} is used simply as a descriptor of the atomic ratio of lithium to sulfur. Solutions were mixed for at least 24 h at 90 °C in a sealed vial within an argon-filled glovebox.

Solution sulfur concentrations (referred to as C_S) used here represent the overall atomic moles of sulfur per volume of solution. For instance, a 10 mM concentration solution contains 10 mmol of atomic S per liter of solution. The millimoles of S atoms represents the sulfur added in the form of S_8 and Li_2S.

To maintain consistent x_{mix} values throughout the study, "bulk", high-concentration solutions were made for each x_{mix} value which were then used to produce the lower concentration solutions through dilution. For instance, the TEGDME $x_{mix} = 6$ solutions were made by first preparing a bulk $x_{mix} = 6$, 300 mM solution. This 300 mM solution was then diluted to create the 100, 50, and 10 mM solutions. This procedure was used for all x_{mix} values. Additions of TEGDME and PEO were performed using a micropipette.

UV−Vis Spectroscopy. Liquid lithium polysulfide solutions were loaded into quartz cuvette sample holders inside an argon-filled glovebox. The quartz cuvettes had a path width of 1 mm. After loading, the cuvettes were sealed and then placed in closed vials with Teflon tape wrapped between the glass threading of the vial and the cap. The vials were then brought out of the glovebox and to the UV−vis spectrophotometer. There cuvettes containing the samples were taken out of the vials and immediately measured. An Agilent Cary 5000 UV−vis−NIR spectrophotometer was used to measure the samples in a range of wavelengths spanning 200−820 nm. Data were obtained in transmission mode. Within the range of sulfur concentrations probed here (C_S = 10, 50, and 100 mM), absorbance spectra became oversaturated below 300 nm. For that reason, our analysis of the UV−vis results is restricted only to the absorbance above 300 nm for all samples. This is of importance given that the absorbance of elemental sulfur occurs in the 200−300 nm range.[9] The measured spectra thus may not represent all of the sulfur-containing species in the samples. Measurement of 300 mM sulfur concentration solutions was attempted, but spectra were oversaturated in the 200−820 nm wavelength range. Spectra were taken for each solvent (TEGDME and PEO); solvent spectra were subtracted from the polysulfide solution spectra shown throughout the rest of this paper. All solutions were measured at room temperature.

Electron Paramagnetic Resonance Spectroscopy. Lithium polysulfide solutions were loaded into borosilicate capillary tubes obtained from Active Spectrum, having an outer diameter of 2.3 mm. Roughly 0.1 mL of solution was loaded into each capillary tube. This volume surpassed the volume of solution present in the measurement cavity of the EPR instrument, meaning that the sample geometry and total solution volume probed for each measurement were identical from sample to sample. Capillary tubes were sealed using a Cha-seal tube sealing compound. The small capillary tubes were then placed inside larger 5 mm outer diameter quartz tubes (Wilmad-LabGlass) that were capped with standard NMR tube caps. Kapton tape was then wrapped around the top of the tube and over the cap to ensure an airtight seal. All sample preparation was performed in an argon-filled glovebox.

Continuous wave (CW) EPR was performed in the X-band frequency range, approximately 9.69 GHz, using an Active Spectrum extended range benchtop EPR instrument. All spectra were obtained at room temperature. The microwave power was set to be 15 mW for all samples. This power was in the linear regime of the power saturation curve obtained for the samples, indicating a quantitative relationship between the double integral of the EPR peaks and sample concentration. The magnetic field had a modulation frequency of 100 kHz and a modulation amplitude of 2 G. Spectra were taken between 2900 and 3900 G at a sweep rate of 7.18 G/s. Two batches of samples were prepared for the set of polysulfide solutions (each solution thus had two separately prepared samples). Five scans were performed and averaged together for each sample. The spectra shown herein are the spectra obtained for one of the sample batches. Raw spectra were smoothed using a second-order Savitsky−Golay filter algorithm, with a frame size of 4 G.

DOI: 10.1021/acs.jpcc.6b04264
J. Phys. Chem. C 2016, 120, 18403−18410

Spectra were obtained for the capillary tubes, TEGDME, and PEO. These background spectra were subtracted from the lithium polysulfide mixture spectra.

RESULTS AND DISCUSSION

Figure 1 shows UV−vis spectroscopy results for TEGDME lithium polysulfide solutions at a variety of x_{mix} values and sulfur concentrations (C_S). Here x_{mix} denotes the ratio of sulfur to lithium ($Li_2S_{x_{mix}}$), as described in reaction 1 in the Experimental Section. UV−vis spectra were obtained for x_{mix} values of 4, 6, 8, and 10 and sulfur concentrations of 10, 50, and 100 mM. For ether-based solvents, the peaks in the 300−550 nm range are generally attributed to polysulfide dianions.[8,9,38] The identity of the peak at 617 nm has not been confirmed for ether-based polysulfide solutions. While some have attributed the peak to radical polysulfides,[8,9] others have attributed the peak to polysulfide dianions.[38] Since our primary interest is to characterize radical anions in ether-based solvents, we focus on the peak at 617 nm.

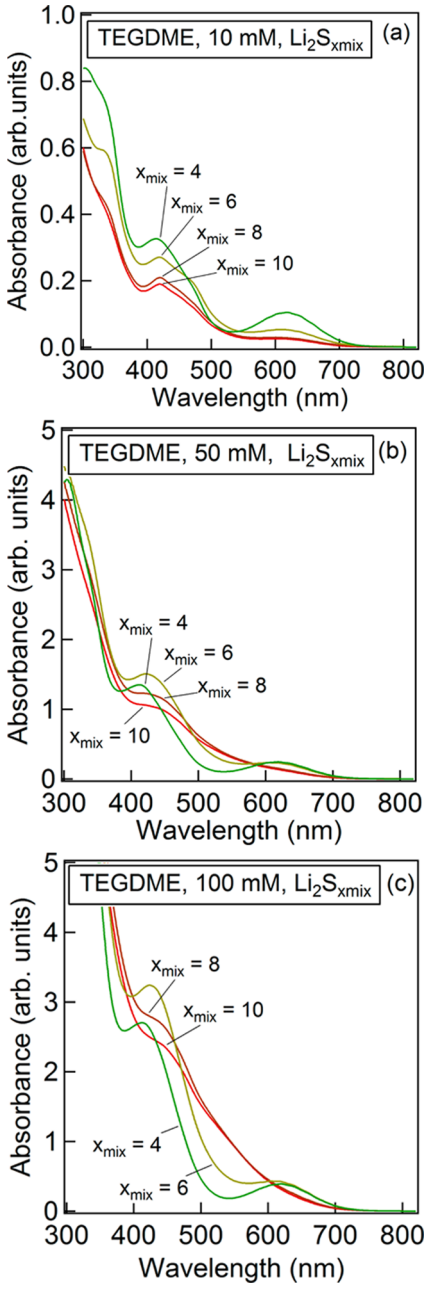

Figure 1. UV−vis spectra obtained for TEGDME lithium polysulfide solutions at sulfur concentrations of (a) 10 mM, (b) 50 mM, and (c) 100 mM. Corresponding colors: x_{mix} = 4 (green), x_{mix} = 6 (yellow), x_{mix} = 8 (brown), x_{mix} = 10 (red).

Table 1. Gaussian Peak Amplitude and Area for the 617 nm UV−Vis Peak at Sulfur Concentrations (C_S) of 10, 50, and 100 mM

	C_S = 10 mM		C_S = 50 mM		C_S = 100 mM	
x_{mix}	amplitude	area	amplitude	area	amplitude	area
4	0.103	12.1	0.242	28.2	0.388	45.1
6	0.049	6.0	0.209	24.5	0.386	45.1
8	0.026	3.4	0.076	9.0	0.124	15.7
10	0.022	2.6	0.062	7.3	0.077	10.0

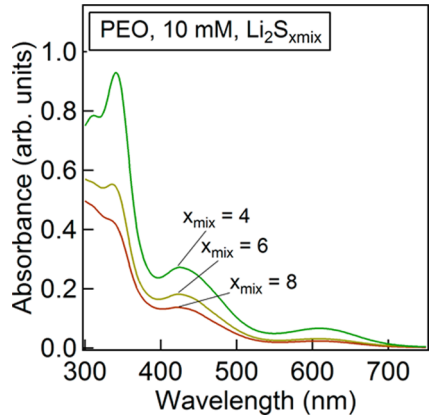

Figure 2. UV−vis spectra obtained for PEO lithium polysulfide (C_S = 10 mM) solutions.

Table 2. Photographs of UV−Vis Cuvettes Filled with TEGDME and PEO Lithium Polysulfide Solutions

TEGDME	x_{mix} value				PEO	x_{mix} value		
Concentration (C_S)	4	6	8	10	Concentration (C_S)	4	6	8
10 mM					10 mM			
50 mM					300 mM			
100 mM	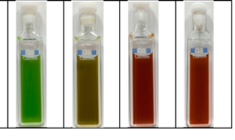							

At a 10 mM sulfur concentration, the x_{mix} = 4 solution has the highest absorbance at 617 nm, followed by x_{mix} = 6, x_{mix} = 8, and x_{mix} = 10. At 50 mM (Figure 1b), x_{mix} = 4 and x_{mix} = 6 appear to have similar absorbances at 617 nm, again followed by x_{mix} = 8 and x_{mix} = 10. At 100 mM (Figure 1c), an identical trend is observed. The highest absorbance at 617 nm in DMF solutions of lithium polysulfides occurs at x_{mix} = 6.[20] Our results for TEGDME are thus slightly different, but consistent with

DOI: 10.1021/acs.jpcc.6b04264
J. Phys. Chem. C 2016, 120, 18403−18410

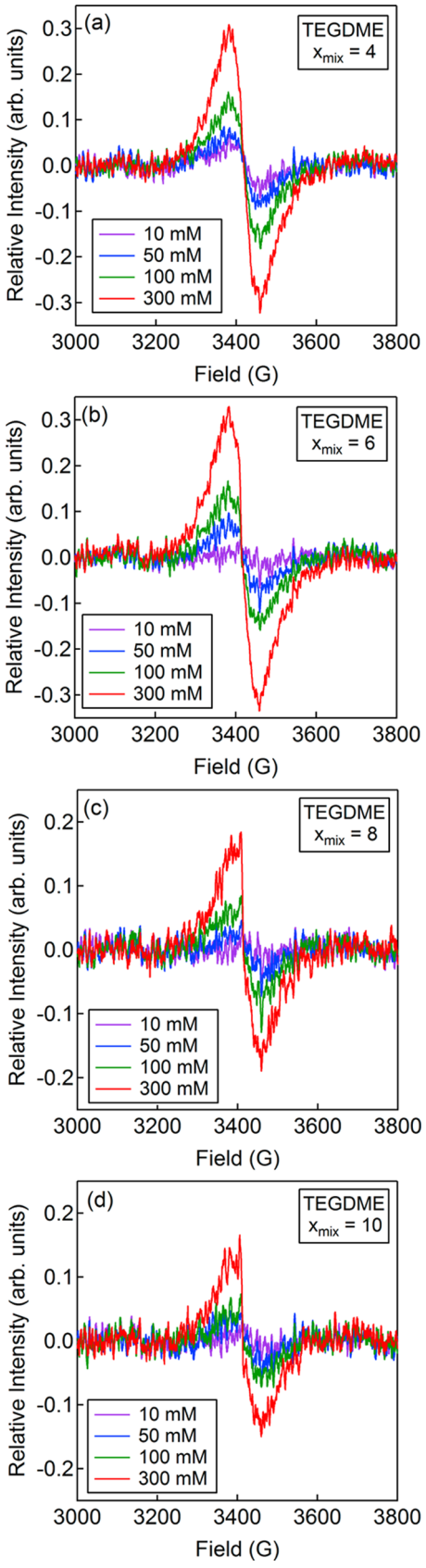

Figure 3. EPR spectra obtained for TEGDME lithium polysulfide solutions for x_{mix} values of (a) 4, (b) 6, (c) 8, and (d) 10 at a range of sulfur concentrations (C_S) between 10 and 300 mM. All spectra were obtained at room temperature.

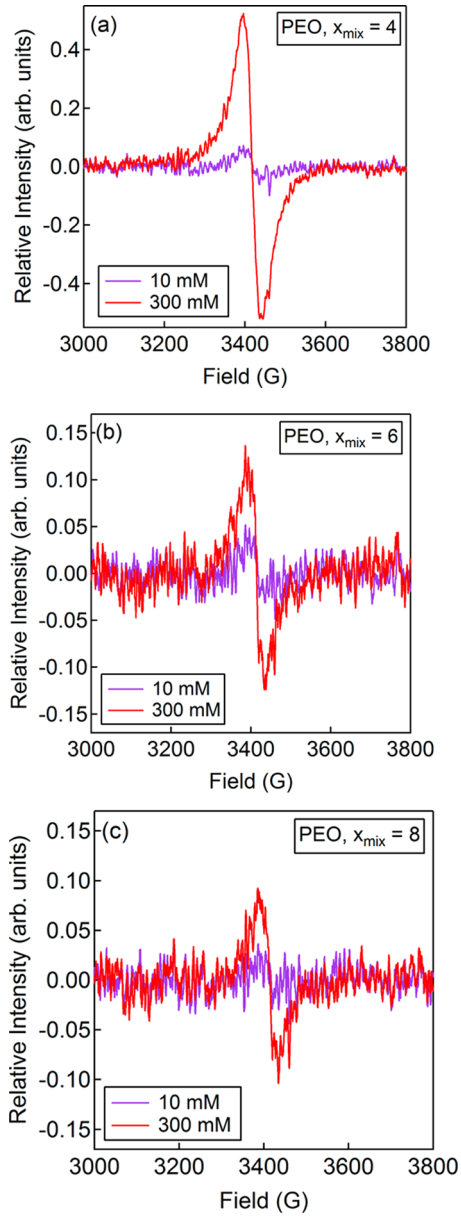

Figure 4. EPR spectra obtained for PEO lithium polysulfide solutions for x_{mix} values of (a) 4, (b) 6, and (c) 8 at sulfur concentrations (C_S) of 10 and 300 mM. All spectra were obtained at room temperature.

data obtained for DMF solutions.[20,21] The spectra shown in Figure 1 were fit using a series of Gaussian functions. Results of this fitting procedure for the 617 nm peak are shown in Table 1. (Parameters corresponding to the other peaks are given the in Supporting Information.)

PEO solutions at x_{mix} values of 4, 6, and 8 at a concentration of 10 mM were also examined using UV−vis spectroscopy. The resulting spectra for these solutions are shown in Figure 2. Similar to the results obtained for TEGDME, the x_{mix} = 4 solution shows the largest absorbance at 617 nm, followed by x_{mix} = 6 and x_{mix} = 8.

Polysulfide mixtures in DMF, DMSO, and like solvents are typically blue in color.[3,12,18,23] Photographs of the TEGDME and PEO solutions examined in this study are shown in Table 2. TEGDME solutions with x_{mix} values equal to 4 were green in color for all concentrations. For x_{mix} = 6, solutions were light yellow/green at 10 mM, and then became a dark olive/brown

DOI: 10.1021/acs.jpcc.6b04264
J. Phys. Chem. C 2016, 120, 18403−18410

Table 3. Peak Areas Obtained by Double Integration of TEGDME and PEO EPR Spectra for x_{mix} = 4, 6, 8, and 10 at Sulfur Concentrations (C_S) of 10, 50, 100, and 300 mM

	TEGDME double integral (arbitrary units)				PEO double integral (arbitrary units)	
x_{mix}	C_S = 10 mM	C_S = 50 mM	C_S = 100 mM	C_S = 300 mM	C_S = 10 mM	C_S = 300 mM
4	328 ± 218	740 ± 13	1797 ± 59	3797 ± 702	140 ± 106	2389 ± 1735
6	108 ± 70	632 ± 133	1536 ± 25	4438 ± 78	35 ± 49	510 ± 214
8	35 ± 25	329 ± 185	574 ± 131	1668 ± 200	17 ± 15	294 ± 110
10	23 ± 15	203 ± 3	337 ± 124	1216 ± 218		

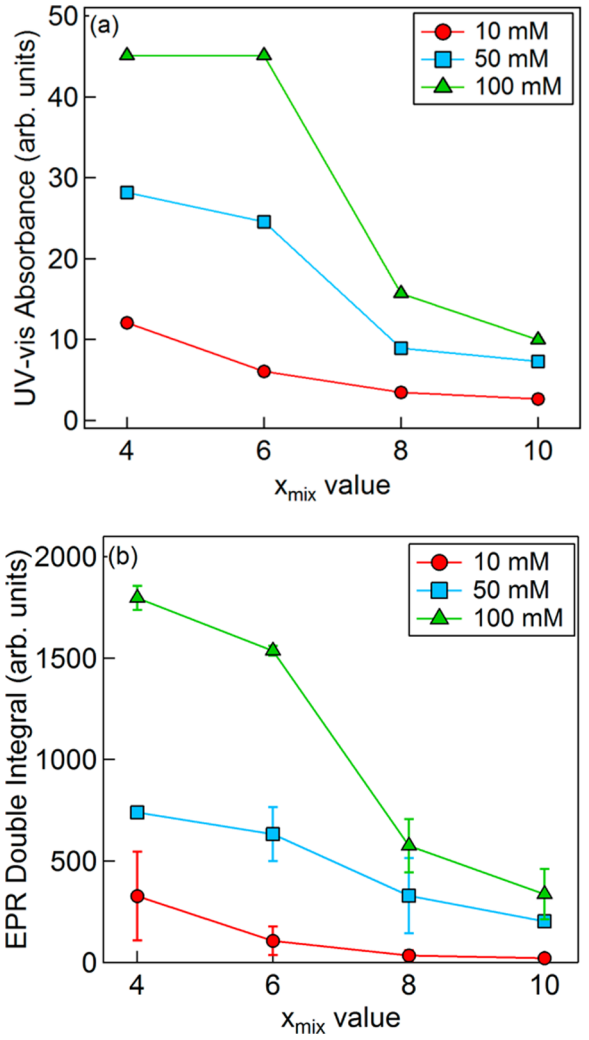

Figure 5. (a) Peak area obtained for the UV−vis 617 nm absorbance peak and (b) double integral of the EPR spectra as a function of the lithium to sulfur ratio (x_{mix}) at sulfur concentrations (C_S) between 10 and 100 mM. Lines connecting the data points are provided as a guide for the eye.

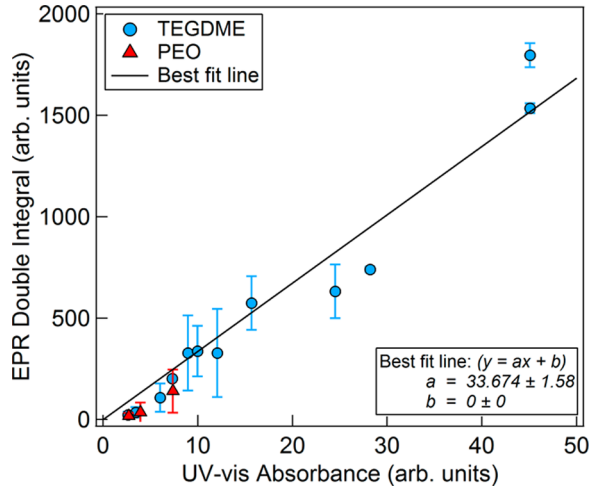

Figure 6. UV−vis peak area (617 nm) versus the double integral of the EPR spectra for TEGDME and PEO solutions. Peak areas obtained from UV−vis and the EPR double integrals are proportional, indicating a direct relationship between the 617 nm UV−vis feature and the presence of radical anions.

color at high concentrations. The x_{mix} = 8 solutions were light yellow/green in color at 10 mM, orange/brown at 50 mM, and dark red at 100 mM. The x_{mix} = 10 solutions were light yellow at 10 mM, orange/brown at 50 mM, and dark red at 100 mM. Low concentration x_{mix} = 4 PEO solutions were light green/yellow at low concentrations and dark yellow/brown at higher concentrations, x_{mix} = 6 solutions were light yellow at low concentration and red at higher concentrations, and x_{mix} = 8 solutions were light yellow at low concentration and red at higher concentration.

While the attribution of the 617 nm peak in the UV−vis spectra to a radical anion is consistent with what has been established for DMF and DMSO, the TEGDME and PEO solutions are not blue in color, as is typically the case for radical-containing polysulfide solutions. The low EPD number of TEGDME and PEO (compared to DMF and DMSO), and lack of blue color in these solutions, thus brings to question whether the 617 nm peak truly represents a radical anion.

Figures 3 and 4 show the EPR spectra obtained for TEGDME and PEO solutions, respectively, at a variety of x_{mix} values and concentrations. Radical species are detected in all TEGDME and PEO solutions at the range of concentrations probed. Additionally, the concentration of radical species increased as the sulfur concentration increased, which is most clearly shown by the x_{mix} = 4 and 6 TEGDME solutions (Figure 3a,b).

To obtain more insight regarding the behavior of the EPR spectra in relation to the concentration and x_{mix} value, the EPR spectra were fit using a Tsallian first-derivative peak function, which was then double integrated to obtain an integrated peak area (here referred to as the "double integral") proportional to the overall concentration of radical species present.[43] Integration of the Tsallian fitting reduces the error due to noise and unsteady baselines in the raw data.[44,45] (Additional spin-counting experiments necessary to obtain absolute radical concentrations by EPR were not attempted.) Our analysis enables a comparison of radical concentrations in the solutions of interest. The results of the peak fitting are summarized in Table 3. The fitting of each spectrum and detailed parameters for each Tsallian fit can be found in the Supporting

DOI: 10.1021/acs.jpcc.6b04264
J. Phys. Chem. C 2016, 120, 18403−18410

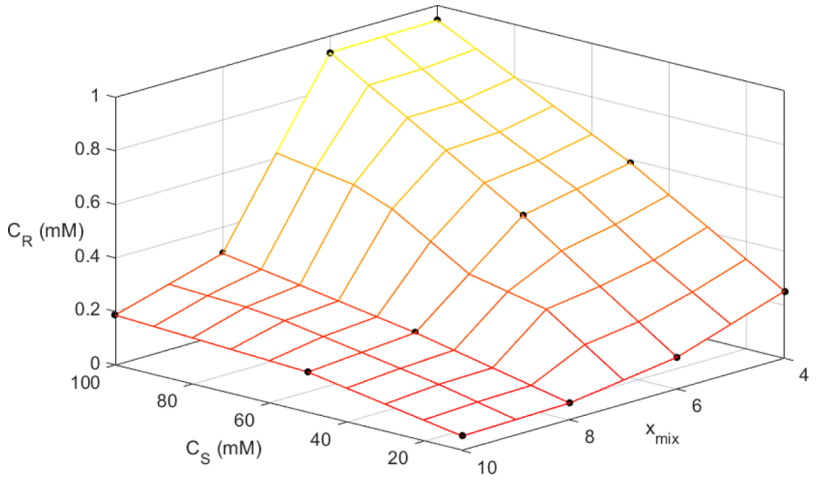

Figure 7. Polysulfide radical anion concentrations (C_R) determined by applying the Beer–Lambert law to the 617 nm peak of the TEGDME UV–vis spectra. The radical concentration is plotted against C_S, the concentration of atomic sulfur, and x_{mix} ($Li_2S_{x_{mix}}$). Data points for polysulfide solutions are shown as black circles, and the surface mesh was calculated via linear interpolation. Yellow indicates a high concentration of radical species, while red denotes a low concentration of radical species.

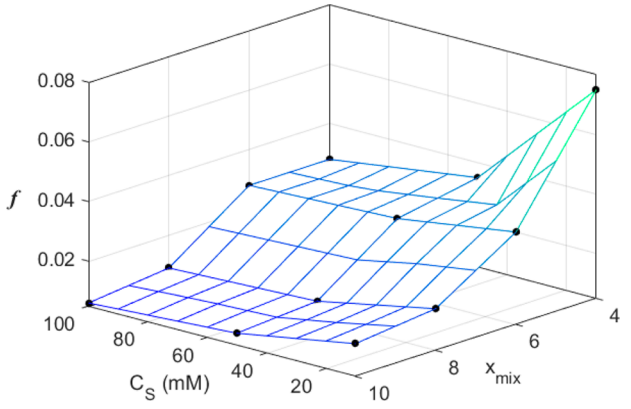

Figure 8. Estimated fraction of sulfur present as radical species (f) in TEGDME plotted against C_S, the concentration of atomic sulfur, and x_{mix} ($Li_2S_{x_{mix}}$). Data points for polysulfide solutions are shown as black circles, and the surface mesh was calculated via linear interpolation. Green indicates the highest fraction of radical species, while blue/purple denotes a lower fraction of radical species.

Information. It is worth noting that while a Tsallian line shape could be fit to the TEGDME x_{mix} = 6, x_{mix} = 8, and x_{mix} = 10, 10 mM spectra, the poor signal-to-noise ratio of these spectra introduces significant error in the relative concentration of radical species measured in these low sulfur concentration samples, as can be seen from the large errors in the 10 mM column of Table 3. Additionally, the noise present in these spectra made it difficult to obtain reliable g factors for these solutions. Thus, the 10 mM solutions were omitted from the calculation of the TEGDME and PEO average g factors.

The average g factor obtained for the TEGDME solutions was 2.0294 ± 0.0011, while that obtained for the PEO solutions was 2.0323 ± 0.0021. A comprehensive list of each solution's g factor can be found in the Supporting Information. These g factors are similar to those previously obtained for the $S_3^{\bullet-}$ radical (2.029)[7,12,18,20,28,46] and the $S_4^{\bullet-}$ radical (2.031).[21] Conclusive identification of the radicals present in the TEGDME and PEO solutions will be a focus of future work, as it is difficult to determine given the broad line width and low signal-to-noise ratio of the spectra. For now, the general agreement between g factors obtained here and those previously obtained for polysulfide solutions serves to show that the radical species elucidated by EPR are most likely polysulfide species.

The EPR results show that radical species are certainly present in the TEGDME and PEO polysulfide solutions, despite their green, red, and brown colors and despite their low EPD numbers. Other researchers have also detected polysulfide radicals in ether-based solvents by EPR.[7] However, the correspondence between EPR signals and UV–vis data for ether-based polysulfide solutions has not been established. We do this in Figure 5. In Figure 5a, we plot the peak areas obtained at the 617 nm UV–vis wavelength versus the x_{mix} value for three concentrations. In Figure 5b, we plot the peak area obtained by double integration of the EPR spectra versus x_{mix} for the same concentrations. The lines connecting the data points in Figure 5 are presented only as a guide for the eye. The trends observed in Figure 5 are nearly identical. Furthermore, we plot the UV–vis peak areas versus the EPR double integral in Figure 6. To a first approximation, the UV–vis 617 nm peak area is directly proportional to the EPR double integral. It is evident that the UV–vis peak at 617 nm of TEGDME and PEO solutions is due to the presence of polysulfide radical anions.

To gain insight into the concentration of radical species present in the TEGDME polysulfide solutions, the UV–vis data were used to calculate radical concentrations according to the Beer–Lambert law:

$$A = \varepsilon C_R l \tag{2}$$

Here the absorbance, A, is taken to be the absorbance value at the 617 nm peak maximum, C_R is the concentration of radical species present, l is the path length within the cuvette, and ε is the absorption coefficient at 617 nm. We used an absorption coefficient of 4115 M^{-1} cm^{-1}, as previously obtained by Levillain et al.[20] The radical concentration calculated for each TEGDME solution is plotted in Figure 7 as a function of the sulfur concentration (C_S) and x_{mix}.

Figure 7 shows that the polysulfide radical concentration is a complex function of C_S and x_{mix}. In general, the radical concentration increases with C_S, but the increase is dramatic for

DOI: 10.1021/acs.jpcc.6b04264
J. Phys. Chem. C 2016, 120, 18403–18410

low values of x_{mix} (e.g., x_{mix} = 4). At constant C_S, the radical concentration (C_R) is a sigmoidal function of x_{mix}, increasing rapidly in the vicinity of x_{mix} = 7. The fact that the radical concentration increases with the sulfur concentration is not surprising. One can use these data to elucidate the fraction of sulfur present as radical species in these solutions, *f*. To do this, one needs information about the distribution of radical anions in solutions. While conclusive identification of the radical species present in the TEGDME solutions will be a focus of future work, we calculate *f* assuming that the radical species were present in the form of LiS_3. This assumption is supported by the similarity of the EPR *g* factors obtained for the TEGDME solutions and those previously obtained for LiS_3. One may thus view *f* as a crude estimate of the fraction of sulfur atoms in radical form:

$$f = \frac{3C_R}{C_S} \tag{3}$$

This fraction, *f*, calculated according to eq 3, is plotted in Figure 8 as a function of the sulfur concentration (C_S) and x_{mix}.

The values of *f* lie between 0.005 and 0.080 depending on the sulfur concentration and lithium to sulfur ratio. The radical fraction, *f*, is highest at low values of x_{mix} and low sulfur concentrations. The physiochemical properties of lithium polysulfide solutions will depend on both C_R and *f*; solutions with large *f* have low values of C_R. The increase of *f* with decreasing C_S is consistent with what has previously been observed in DMF solutions, and is evidence of the dianion/radical anion dissociation equilibrium.[3] Radical species are favored at low concentrations, while recombination of radicals to form dianion polysulfides is favored at higher sulfur concentrations.

CONCLUSIONS

We conclude that polysulfide radical anions are present in ether-based solvents, TEGDME and PEO. This conclusion is based on both UV−vis and EPR spectroscopy. We demonstrate quantitative relationships between the UV−vis and EPR signals in our solutions. We determine both the total radical concentration and fraction of sulfur in radical form. These parameters are complex functions of the sulfur concentration and lithium to sulfur ratio, as shown in Figures 7 and 8. The fraction of radical species is high in dilute solutions and when the lithium to sulfur ratio is high.

ASSOCIATED CONTENT

Supporting Information

The Supporting Information is available free of charge on the ACS Publications website at DOI: 10.1021/acs.jpcc.6b04264.

Parameters and description for fitting of UV−vis and EPR spectra as well as EPR *g* factors (PDF)

AUTHOR INFORMATION

Corresponding Author

*E-mail: nbalsara@berkeley.edu. Phone: (510) 642-8937.

Notes

The authors declare no competing financial interest.

ACKNOWLEDGMENTS

This work was supported by the Assistant Secretary for Energy Efficiency and Renewable Energy, Office of Vehicle Technologies of the U.S. Department of Energy under Contract DE-AC02-05CH11231 under the Battery Materials Research program. UV−vis spectroscopy was performed under a User Project at The Molecular Foundry. We thank Professor Jeffrey Reimer for enabling the EPR experiments and Eric Scott for his support and useful discussions regarding EPR.

NOMENCLATURE

Li−S	lithium sulfur
TEGDME	tetraethylene glycol dimethyl ether
PEO	poly(ethylene oxide)
EPR	electron paramagnetic resonance
UV−vis	ultraviolet−visible
EPD	electron pair donor
DMF	dimethylformamide
DMSO	dimethyl sulfoxide
THF	tetrahydrafuran
XAS	X-ray absorption spectroscopy
DME	dimethyl ether
DOL	dioxolane
x_{mix}	ratio of lithium to sulfur
C_S	sulfur concentration (mM)
NIR	near-infrared
NMR	nuclear magnetic resonance
CW	continuous wave
G	gauss
A	absorbance
ε	absorption coefficient
C_R	radical concentration
L	path length of the UV−vis cuvette
f	fraction of atomic sulfur in the form of radicals

REFERENCES

(1) Bruce, P. G.; Freunberger, S. A.; Hardwick, L. J.; Tarascon, J.-M. Li-O2 and Li-S Batteries with High Energy Storage. *Nat. Mater.* **2012**, *11*, 19−29.

(2) Rauh, R. D.; Abraham, K. M.; Pearson, G. F.; Surprenant, J. K.; Brummer, S. B. A Lithium/Dissolved Sulfur Battery with an Organic Electrolyte. *J. Electrochem. Soc.* **1979**, *126*, 523−527.

(3) Rauh, R. D.; Shuker, F. S.; Marston, J. M.; Brummer, S. B. Formation of Lithium Polysulfides in Aprotic Media. *J. Inorg. Nucl. Chem.* **1977**, *39*, 1761−1766.

(4) Mikhaylik, Y. V.; Akridge, J. R. Polysulfide Shuttle Study in the Li/S Battery System. *J. Electrochem. Soc.* **2004**, *151*, A1969−A1976.

(5) Manthiram, A.; Fu, Y.; Chung, S.-H.; Zu, C.; Su, Y.-S. Rechargeable Lithium−Sulfur Batteries. *Chem. Rev.* **2014**, *114*, 11751−11787.

(6) Yin, Y.-X.; Xin, S.; Guo, Y.-G.; Wan, L.-J. Lithium−Sulfur Batteries: Electrochemistry, Materials, and Prospects. *Angew. Chem., Int. Ed.* **2013**, *52*, 13186−13200.

(7) Wang, Q.; et al. Direct Observation of Sulfur Radicals as Reaction Media in Lithium Sulfur Batteries. *J. Electrochem. Soc.* **2015**, *162*, A474−A478.

(8) Barchasz, C.; Molton, F.; Duboc, C.; Lepretre, J. C.; Patoux, S.; Alloin, F. Lithium/Sulfur Cell Discharge Mechanism: An Original Approach for Intermediate Species Identification. *Anal. Chem.* **2012**, *84*, 3973−80.

(9) Cañas, N. A.; Fronczek, D. N.; Wagner, N.; Latz, A.; Friedrich, K. A. Experimental and Theoretical Analysis of Products and Reaction Intermediates of Lithium−Sulfur Batteries. *J. Phys. Chem. C* **2014**, *118*, 12106−12114.

(10) Cuisinier, M.; Hart, C.; Balasubramanian, M.; Garsuch, A.; Nazar, L. F. Radical or Not Radical: Revisiting Lithium−Sulfur Electrochemistry in Nonaqueous Electrolytes. *Adv. Energy Mater.* **2015**, *5*, 1401801.

DOI: 10.1021/acs.jpcc.6b04264
J. Phys. Chem. C 2016, 120, 18403−18410

(11) Wujcik, K. H.; Pascal, T. A.; Pemmaraju, C. D.; Devaux, D.; Stolte, W. C.; Balsara, N. P.; Prendergast, D. Characterization of Polysulfide Radicals Present in an Ether-Based Electrolyte of a Lithium−Sulfur Battery During Initial Discharge Using in Situ X-Ray Absorption Spectroscopy Experiments and First-Principles Calculations. *Adv. Energy Mater.* **2015**, *5*, 1500285.
(12) Seel, F.; Güttler, H. J.; Simon, G.; Wieckowski, A. Colored Sulfur Species in EPD-Solvents. *Pure Appl. Chem.* **1977**, *49*, 45−54.
(13) Dokko, K.; et al. Solvate Ionic Liquid Electrolyte for Li−S Batteries. *J. Electrochem. Soc.* **2013**, *160*, A1304−A1310.
(14) Chivers, T.; Elder, P. J. W. Ubiquitous Trisulfur Radical Anion: Fundamentals and Applications in Materials Science, Electrochemistry, Analytical Chemistry and Geochemistry. *Chem. Soc. Rev.* **2013**, *42*, 5996−6005.
(15) Fleet, M. E.; Liu, X. X-Ray Absorption Spectroscopy of Ultramarine Pigments: A New Analytical Method for the Polysulfide Radical Anion S3− Chromophore. *Spectrochim. Acta, Part B* **2010**, *65*, 75−79.
(16) Steudel, R. *Elemental Sulfur and Sulfur-Rich Compounds II*; Springer: Berlin, Heidelberg, 2003; Vol. *231*.
(17) Reinen, D.; Lindner, G.-G. The Nature of the Chalcogen Colour Centres in Ultramarine-Type Solids. *Chem. Soc. Rev.* **1999**, *28*, 75−84.
(18) Clark, R. J. H.; Cobbold, D. G. Characterization of Sulfur Radical Anions in Solutions of Alkali Polysulfides in Dimethylformamide and Hexamethylphosphoramide and in the Solid State in Ultramarine Blue, Green, and Red. *Inorg. Chem.* **1978**, *17*, 3169−3174.
(19) Giggenbach, W. On the Nature of the Blue Solutions of Sulfur. *J. Inorg. Nucl. Chem.* **1968**, *30*, 3189−3201.
(20) Leghie, P.; Levillain, E.; Lelieur, J. P.; Lorriaux, A. Spectroscopic Study of Lithium Hexasulfide Solutions in DMF. *New J. Chem.* **1996**, *20*, 1121−1130.
(21) Levillain, E.; Leghie, P.; Gobeltz, N.; Lelieur, J. P. Identification of the S4- Radical Anion in Solution. *New J. Chem.* **1997**, *21*, 335−341.
(22) Bonnaterre, R.; Cauquis, G. Spectrophotometric Study of the Electrochemical Reduction of Sulphur in Organic Media. *J. Chem. Soc., Chem. Commun.* **1972**, 293−294.
(23) Chivers, T.; Drummond, I. Characterization of the Trisulfur Radical Anion S3- in Blue Solutions of Alkali Polysulfides in Hexamethylphosphoramide. *Inorg. Chem.* **1972**, *11*, 2525−2527.
(24) Gaillard, F.; Levillain, E. Visible Time-Resolved Spectroelectrochemistry: Application to Study of the Reduction of Sulfur (S8) in Dimethylformamide. *J. Electroanal. Chem.* **1995**, *398*, 77−87.
(25) Gaillard, F.; Levillain, E.; Dhamelincourt, M. C.; Dhamelincourt, P.; Lelieur, J. P. Polysulphides in Dimethylformamide: A Micro-Raman Spectroelectrochemical Study. *J. Raman Spectrosc.* **1997**, *28*, 511−517.
(26) Gaillard, F.; Levillain, E.; Lelieur, J. P. Polysulfides in Dimethylformamide: Only the Radical Anions S3− and S4− Are Reducible. *J. Electroanal. Chem.* **1997**, *432*, 129−138.
(27) Han, D.-H.; Kim, B.-S.; Choi, S.-J.; Jung, Y.; Kwak, J.; Park, S.-M. Time-Resolved in Situ Spectroelectrochemical Study on Reduction of Sulfur in N,N ′-Dimethylformamide. *J. Electrochem. Soc.* **2004**, *151*, E283−E290.
(28) Kim, B. S.; Park, S. M. In Situ Spectroelectrochemical Studies on the Reduction of Sulfur in Dimethyl Sulfoxide Solutions. *J. Electrochem. Soc.* **1993**, *140*, 115−122.
(29) Levillain, E.; Gaillard, F.; Leghie, P.; Demortier, A.; Lelieur, J. P. On the Understanding of the Reduction of Sulfur (S8) in Dimethylformamide (Dmf). *J. Electroanal. Chem.* **1997**, *420*, 167−177.
(30) Levillain, E.; Gaillard, F.; Lelieur, J. P. Polysulfides in Dimethylformamide: Only the Redox Couples S−N/S2−N Are Involved. *J. Electroanal. Chem.* **1997**, *440*, 243−250.
(31) Martin, R. P.; Doub, W. H.; Roberts, J. L.; Sawyer, D. T. Electrochemical Reduction of Sulfur in Aprotic Solvents. *Inorg. Chem.* **1973**, *12*, 1921−1925.
(32) Merritt, M. V.; Sawyer, D. T. Electrochemical Reduction of Elemental Sulfur in Aprotic Solvents. Formation of a Stable S8-Species. *Inorg. Chem.* **1970**, *9*, 211−215.
(33) Paris, J.; Plichon, V. Electrochemical Reduction of Sulphur in Dimethylacetamide. *Electrochim. Acta* **1981**, *26*, 1823−1829.
(34) Tobishima, S.-I.; Yamamoto, H.; Matsuda, M. Study on the Reduction Species of Sulfur by Alkali Metals in Nonaqueous Solvents. *Electrochim. Acta* **1997**, *42*, 1019−1029.
(35) Lowe, M. A.; Gao, J.; Abruna, H. D. Mechanistic Insights into Operational Lithium-Sulfur Batteries by in Situ X-Ray Diffraction and Absorption Spectroscopy. *RSC Adv.* **2014**, *4*, 18347−18353.
(36) Patel, M. U. M.; Arčon, I.; Aquilanti, G.; Stievano, L.; Mali, G.; Dominko, R. X-Ray Absorption near-Edge Structure and Nuclear Magnetic Resonance Study of the Lithium−Sulfur Battery and Its Components. *ChemPhysChem* **2014**, *15*, 894−904.
(37) Patel, M. U. M.; Demir-Cakan, R.; Morcrette, M.; Tarascon, J.-M.; Gaberscek, M.; Dominko, R. Li-S Battery Analyzed by Uv/Vis in Operando Mode. *ChemSusChem* **2013**, *6*, 1177−1181.
(38) Patel, M. U. M.; Dominko, R. Application of in Operando Uv/Vis Spectroscopy in Lithium−Sulfur Batteries. *ChemSusChem* **2014**, *7*, 2167−2175.
(39) Wujcik, K. H.; et al. Fingerprinting Lithium-Sulfur Battery Reaction Products by X-Ray Absorption Spectroscopy. *J. Electrochem. Soc.* **2014**, *161*, A1100−A1106.
(40) Cuisinier, M.; Cabelguen, P.-E.; Evers, S.; He, G.; Kolbeck, M.; Garsuch, A.; Bolin, T.; Balasubramanian, M.; Nazar, L. F. Sulfur Speciation in Li−S Batteries Determined by Operando X-Ray Absorption Spectroscopy. *J. Phys. Chem. Lett.* **2013**, *4*, 3227−3232.
(41) Gorlin, Y.; Siebel, A.; Piana, M.; Huthwelker, T.; Jha, H.; Monsch, G.; Kraus, F.; Gasteiger, H. A.; Tromp, M. Operando Characterization of Intermediates Produced in a Lithium-Sulfur Battery. *J. Electrochem. Soc.* **2015**, *162*, A1146−A1155.
(42) Manthiram, A.; Fu, Y.; Su, Y.-S. Challenges and Prospects of Lithium−Sulfur Batteries. *Acc. Chem. Res.* **2013**, *46*, 1125−1134.
(43) Weil, J. A., Bolton, J. R. *Electron Paramagnetic Resonance: Elementary Theory and Practical Applications*, 2nd ed.; John Wiley & Sons, Inc.: Hoboken, NJ, 2007.
(44) Howarth, D. F.; Weil, J. A.; Zimpel, Z. Generalization of the Lineshape Useful in Magnetic Resonance Spectroscopy. *J. Magn. Reson.* **2003**, *161*, 215−221.
(45) Tseitlin, M.; Eaton, S. S.; Eaton, G. R. Uncertainty Analysis for Absorption and First-Derivative Electron Paramagnetic Resonance Spectra. *Concepts Magn. Reson., Part A* **2012**, *40A*, 295−305.
(46) Dubois, P.; Lelieur, J. P.; Lepoutre, G. Identification and Characterization of Lithium Polysulfides in Solution in Liquid-Ammonia. *Inorg. Chem.* **1988**, *27*, 73−80.

DOI: 10.1021/acs.jpcc.6b04264
J. Phys. Chem. C 2016, 120, 18403−18410